Journal of Alloys and Compounds 509 (2011) 5064–5069

Contents lists available at ScienceDirect

Journal of Alloys and Compounds

journal homepage: www.elsevier.com/locate/jallcom

Microwave assisted chemical bath deposited polyaniline films for supercapacitor application

P.R. Deshmukh, S.N. Pusawale, V.S. Jamadade, U.M. Patil, C.D. Lokhande*

Thin Film Physics Laboratory, Department of Physics, Shivaji University, Kolhapur 416004 (M.S.), India

ARTICLE INFO

Article history:
Received 6 September 2010
Received in revised form
30 November 2010
Accepted 1 December 2010
Available online 9 December 2010

Keywords:
Thin films
Chemical synthesis
Microwave assisted chemical bath deposition (MW-CBD)
Wettability test
Optical properties
Supercapacitive behavior

ABSTRACT

In the present investigation, we are reporting the first time synthesis of polyaniline (PANI) thin films by microwave assisted chemical bath deposition (MW-CBD) method on the stainless steel substrate. The PANI thin films are prepared by the oxidation of aniline in the domestic microwave oven working with frequency 2.45 GHz. The PANI thin films are characterized for their structural, morphological and optical studies by means of X-ray diffraction (XRD), Fourier transform infrared (FT-IR) spectroscopy, scanning electron microscopy (SEM) and UV–vis spectrophotometer. The wettability study is carried out by measuring the contact angle. The supercapacitive behavior of PANI electrode is studied in 0.5 M H_2SO_4 using cyclic voltammetric (CV) measurements. The X-ray diffraction pattern showed the films are amorphous. Morphological study revealed PANI thin film is well covered over the entire substrate surface with less overgrown fine spherical granules. The optical band gap of PANI thin film is found to be 2.5 eV. The hydrophilic nature of the PANI thin films is observed from water contact angle measurement. A maximum specific capacitance is found to be 753 F g^{-1} at the scan rate of 5 mV s^{-1}.

1. Introduction

The usage of microwave energy to accelerate the organic reaction is of increasing interest and offers several advantages over the conventional heating techniques. Synthesis of molecules, which normally requires a long time, can be achieved conveniently and rapidly in microwave oven [1]. In the chemical bath deposition method, the metal oxide and chalcogenide thin films need a lot of time for the formation i.e. it requires hours or several tens of hours, therefore chemical bath deposition method is time consuming [2–4].

Therefore, a more rapid and efficient method is required to promote the deposition of thin films. The microwave assisted chemical bath deposition (MW-CBD) is innovative and simple method. This method is used for the synthesis of metal oxide, chalcogenides as well as polyaniline/multi walled carbon nanotube composite powder [5]. In the present study for the first time, this method is used to direct grow PANI thin films on stainless steel substrate. In this case, the molecules in the materials undergo collision and friction because of the interaction between the electric dipoles present in the materials and electric field of microwaves, since the microwaves are the electromagnetic waves. Because of this heat is generated and therefore, heating of the substrate is quick in the microwave oven compared with chemical bath deposition method, where the substrate is heated by heat conduction [6–9]. The use of microwave (MW) heating has recently showing the advantages over traditional techniques due to (a) the characteristics of the grown layers (good adherence and transparency), (b) the simplicity of the technique, (c) the possibility controlling the layer thickness with MW heating time, and (d) the low temperature [10]. Interesting electrical and optical properties exhibited by conducting polymers make them an attractive choice for various technological applications. Conducting polymers offer advantage of low cost comparison with metal oxide and a higher charge density than carbon, these often have good intrinsic auto conductivity. Among the conducting polymers, polyaniline (PANI) is largely investigated and studied for its electrochemical characterization [11,12]. It has gained significant interest in the recent times because of its unique electronic properties, simple synthesis process, high conductivity, environmental stability, good redox reversibility and low cost [13,14]. It displays a wide spectrum of applications such as conductive and antistatic material as corrosion inhibitor, electromagnetic shielding in electronic circuits, electrochromic devices, piezoelectric devices, photoconductors, biosensor and microactuators [15–17]. Potential applications of PANI include capacitors, smart windows, gas separation membranes, sensors, etc. [18,19]. As usual, chemical polymerization is provided by the use of some of the known oxidants, which are able to generate radical cations and other highly reactive species upon interaction with aniline. Once generated, these reactive species

* Corresponding author. Tel.: +91 231 2609225; fax: +91 231 2609233.
E-mail address: l.chandrakant@yahoo.com (C.D. Lokhande).

0925-8388/$ – see front matter © 2010 Elsevier B.V. All rights reserved.
doi:10.1016/j.jallcom.2010.12.009

react with aniline molecules, leading to the growing polymer chains [20].

In the present paper, we report a novel microwave synthesis of PANI thin films on conducting substrates and to our knowledge, this is the first attempt to deposit the PANI thin films. Further, supercapacitive behavior of these films is reported.

2. Experimental

2.1. Materials

The monomer aniline (AR grade), ammonium persulphate (AR grade) and sulphuric acid (AR grade) were used as received without further treatment for the preparation. All of the aqueous solutions were prepared with double distilled water. The stainless steel substrate (Grade 316) was polished with emery polish paper to rough finish.

2.2. Synthesis of PANI

Polyaniline (PANI) thin films were prepared by chemical oxidization of aniline with ammonium persulphate. Appropriate amount of aniline and ammonium persulphate were dissolved in the 2 vol. % H_2SO_4 separately into two 100 ml beakers. The prepared 20 ml aniline solution and 20 ml ammonium persulphate solution in H_2SO_4 were taken in 50 ml glass beaker. The mirror polished steel substrates were placed vertically in precursor solution for the MW-CBD process. The glass beaker containing the precursor solution and substrate was placed in the centre of a second 150 ml beaker filled with 100 ml water. This second container was intended to absorb heat from the precursor solution during processing. The container was placed in the centre of domestic microwave oven cavity on top of the rotating plate. The microwave power was used as 100 W. Continuous microwave irradiation time did not exceed 10 min. The greenish color starts to appear after 5–6 min and after 10 min precipitation forms in the bath. The precursor solution temperature after 10 min microwave irradiation attains the temperature 55 °C. The same process was repeated for five times, to achieve the maximum thickness and well adherent film on the steel substrate (Grade 316) [6], always starting from the room temperature. The prepared thin films were uniformly deposited, well adherent to the substrate and reproducible.

The X-ray diffraction (XRD) pattern was obtained with Philips (PW 3710) diffractometer using CrK_α radiation (λ = 2.28970 Å). Surface morphology was studied with the help of scanning electron microscope (JEOL-6360). For this, the films were coated with a 10 nm platinum layer using a polaron scanning electron microscopy (SEM) sputter coating unit E-2500 before taking the image. Fourier transform infrared (FT-IR) spectroscopy was recorded between 4000 and 450 cm^{-1} at a spectral resolution of 2 cm^{-1} on a PerkinElmer 1710 spectrophotometer using KBr pellets at room temperature. To study the optical characteristic of the film, absorbance spectra were recorded in the range 350–750 nm by means of UV–vis spectrophotometer-119. The electrochemical analysis of the films deposited on stainless steel substrate was studied by cyclic voltammetry (CV) using the potentiostat (263A EG&G, Princeton Applied Research Potentiostat). The electrochemical impedance measurements were conducted with a versaStat 3G frequency response analyzer (FRA) under Zplot program (Scribner Associates Inc.) The charge/discharge analysis was performed by WonATech Automatic Battery Cycler, WBCS3000 system interfaced to a computer.

Thickness measurement was carried out by the gravimetric weight difference method using sensitive microbalance with the relation $t = \Delta m/(\rho A)$, where 'Δm' is weight of the film deposited on the substrate in grams, 'A' is the deposited area of the film in cm^2, and 'ρ' is the density of the deposited material (ρ = 1.30 g cm^{-3}) in bulk form [21]. The maximum thickness obtained for polyaniline thin film was 1.2 μm.

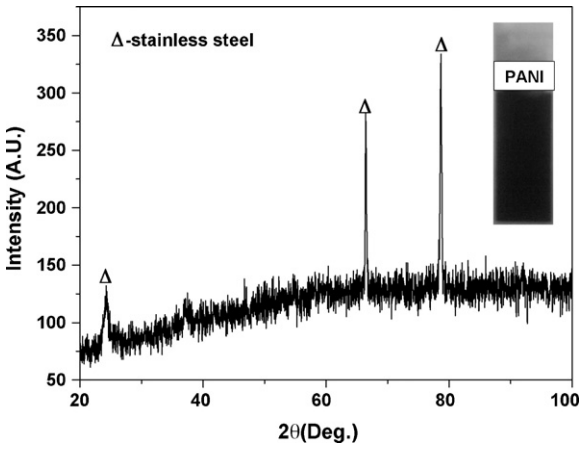

Fig. 1. XRD pattern of PANI thin films deposited on stainless steel substrate. [Inset figure shows the photograph of PANI thin film.]

3. Results and discussion

3.1. Structural analysis

In order to study the structural analysis the XRD patterns of the PANI thin films, were recorded in the 2θ range 20–100°. Fig. 1 shows the XRD pattern of the polyaniline thin film on the stainless steel substrate. The XRD pattern showed the absence of any sharp diffraction lines, indicating the deposited polyaniline thin film is amorphous in nature. The peak observed in the pattern is due to the stainless steel substrate. Such amorphous polyaniline thin films are synthesized using electrodeposition method by Joshi and Lokhande [22]. The inset of Fig. 1 shows the photograph of polyaniline thin film is greenish in color over ~10 cm^2 area (two sides of substrates) confirming the feasibility of MW-CBD method for large area deposition.

3.2. Surface morphological and surface wettability studies

The surface morphology of the PANI thin film was investigated by the scanning electron microscope (SEM) technique. Fig. 2 shows the scanning electron micrographs of the PANI thin films at different magnifications (a) 2000× and (b) 10,000×. At lower magnification of 2000× (Fig. 2a) SEM image shows, PANI is well

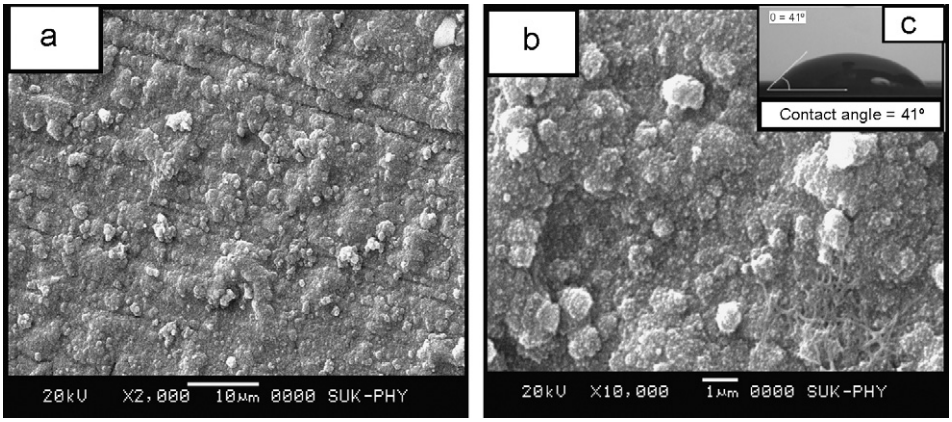

Fig. 2. The scanning electron micrographs and the contact angle measurement of the PANI thin films at (a) 2000× and (b) 10,000× magnifications and (c) water contact angle of surface of the PANI thin films.

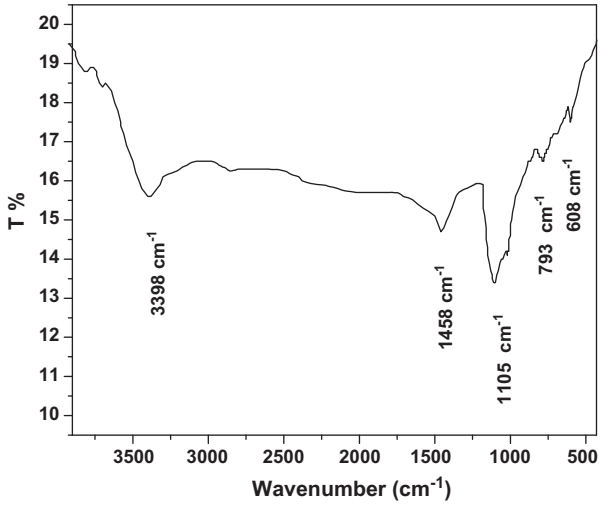

Fig. 3. FT-IR spectrum of PANI thin film.

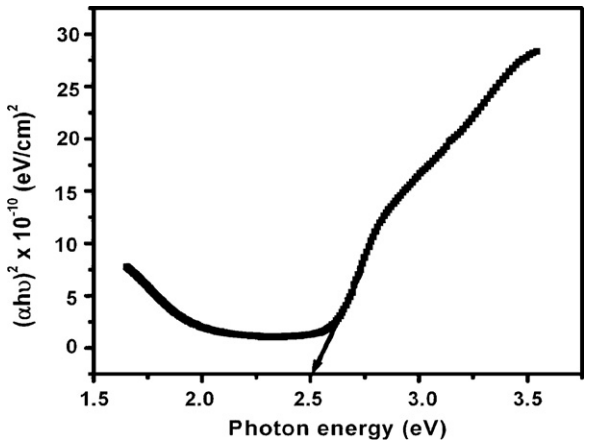

Fig. 4. Plot of $(\alpha h\upsilon)^2$ vs. $h\upsilon$ of the PANI thin film.

covered over the entire substrate surface with less overgrown fine spherical granules. At higher magnification of 10,000× (Fig. 2b), the surface of images shows valley and mountains. From the micrographs, it is revealed that the substrate is fully covered by the nanoparticles. A fine features of material frequently indicate as amorphous or nanocrystalline structure. Hydrophilic nature was observed from the water contact angle measurement using Rame–Hart USA equipment with CCD camera. Wettability test is carried out in order to investigate the interaction between electrolyte and PANI electrode. If the wettability is high, contact angle (θ), will be small and the surface is hydrophilic. On the contrary, if the wettability is low, contact angle (θ), will be large and the surface is hydrophobic. In the present report, water lies with contact of 41° on the surface of PANI electrode shown in inset of Fig. 2c [23]. This may be due to the strong cohesive force between the water droplets and the hydroxide present in the PANI electrode. This hydrophilic property is attributed to the nanocrystalline nature, which is expected to possess a very high surface energy. Nanocrystalline material with hydrophilic nature is one of the prime requirements for supercapacitor electrode material. Hydrophilic nature is useful for making close contact of aqueous electrolyte with film surface in supercapacitor application. It is well known that in electrochemical supercapacitor, hydrophilic surface of the electrode is an essential factor for better performance. Mane et al. reported a contact angle 21° for electrochemically deposited tin oxide thin films for supercapacitor application [24,25].

3.3. FT-IR and optical studies

Fig. 3 shows the FT-IR spectrum of the PANI thin film in the range of 4000–450 cm^{-1}. The very weak and broad band at 3398 cm^{-1} is assigned to N–H stretching mode [26]. The peak at 1458 cm^{-1} is attributed to the C=C stretching of benzenoid rings. The peaks at 1105, 793 and 608 cm^{-1} are attributed to bands characteristics of B–NH–Q or B–NH–B bonds, and out of plane bending vibration of C–H of benzene rings, respectively (where B refers to the benzenic-type rings and Q refers to the quinonic-type rings), which confirms the formation of the PANI over substrate [27–30].

The optical properties of the PANI thin films are carried out by UV–vis spectrophotometer. Fig. 4 shows the plot of $(\alpha h\upsilon)^2$ vs. $h\upsilon$ of PANI thin film. The band gap of the polyaniline thin films was found to be 2.5 eV, which is comparable with earlier reports [31].

3.4. Supercapacitive behavior study

The supercapacitive performance of PANI thin film was studied using cyclic voltammetry within the potential range of −0.2 to +0.8 V vs. SCE in 0.5 M H_2SO_4 electrolyte. The effect of scan rate variation is shown in Fig. 5. It was found that the current under curve is slowly increased with scan rate. The capacitance was calculated using the relation

$$C = \frac{I}{d\nu/dt} \quad (1)$$

where 'I' is the average current in amperes and $d\nu/dt$ is the voltage scanning rate. The specific capacitance of polyaniline was obtained by dividing its respective weight using the relation

$$C_s = \frac{C}{W} \quad (2)$$

where 'W' the is weight of the active material on the substrate. The interfacial capacitance was calculated using the relation

$$C_i = \frac{C}{A} \quad (3)$$

where 'A' is the area of active material dipped in the electrolyte. This showed that voltammetric currents are directly proportional to the scan rate of CV, indicating an ideally capacitive behavior [32,33]. The PANI thin film exhibited the specific capacitance 753 F g^{-1}

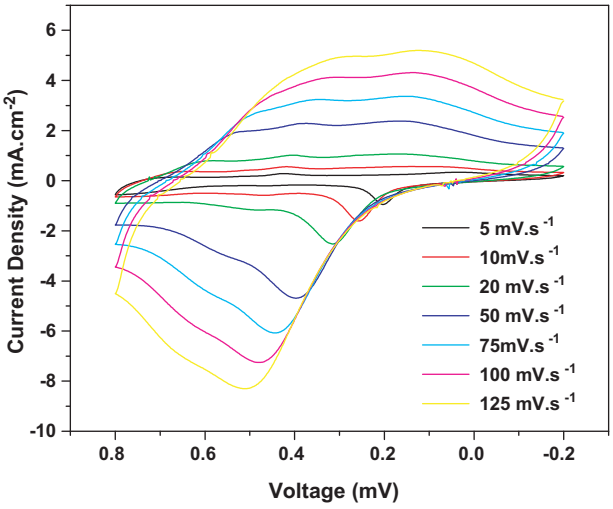

Fig. 5. The CV curves of PANI thin films at various scan rates using 0.5 M H_2SO_4 electrolyte in the potential range of −0.2 to +0.8 V vs. SCE.

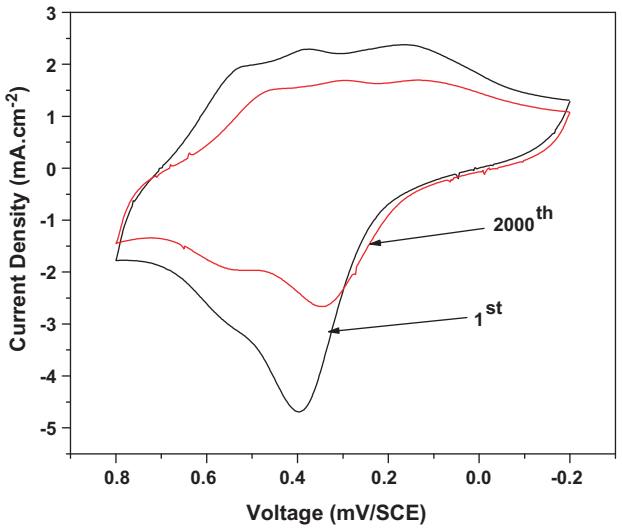

Fig. 6. The CV curves of PANI electrode at different number of cycles. The scanning rate and concentration of H_2SO_4 were 5 mV s^{-1} and 0.5 M H_2SO_4, respectively.

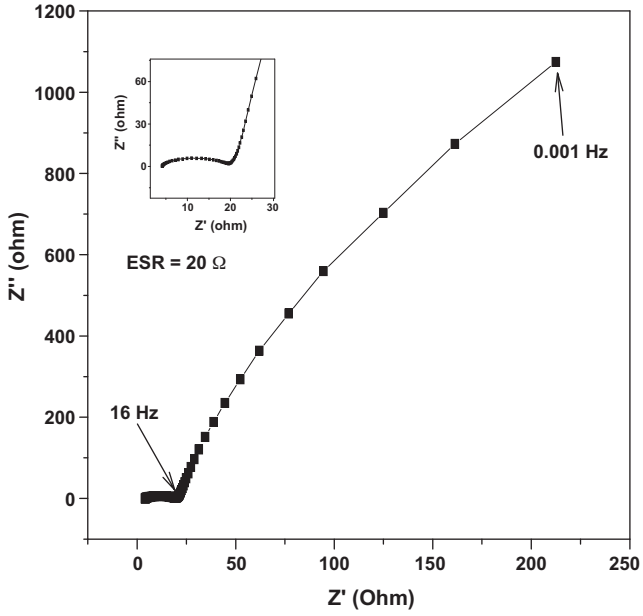

Fig. 7. Nyquist plot of PANI electrode in 0.5 M H_2SO_4 electrolyte.

and interfacial capacitance 0.0640 F cm^{-2} at the scan rate 5 mV s^{-1}. However, it is noteworthy that the supercapacitance of PANI thin film prepared by MW-CBD method is comparable/slightly higher with respect to other methods. Dhawale et al. reported 839 F g^{-1} specific capacitance of PANI electrodes prepared by electrodeposition method [21]. Gupta and Miura reported 742 F g^{-1} specific capacitance of PANI electrodes prepared by electrodeposition method [34]. Jamadade et al. reported 258 F g^{-1} specific capacitance of PANI electrodes prepared by electrodeposition method [35]. However, MW-CBD deposited PANI films showed 753 F g^{-1} specific capacitance since the specific capacitance depends on the morphology and deposition method. The specific and interfacial capacitance values decreased from 753 F g^{-1} to 317 F g^{-1} and 0.0640 F cm^{-2} to 0.0270 F cm^{-2}, respectively as the scan rate increased from the 5 to 125 mV s^{-1}. The decrease in capacitance is attributed to the presence of inner active sites that cannot sustain the redox transitions completely at higher scan rates. This is probably due to the diffusion effect of protons within the electrode. The decreasing capacitance suggests that parts of the surface of the electrode are inaccessible at high charging–discharging rates. Hence, the specific capacitance obtained at the slowest scan rate is believed to be closest to that of full utilization of the electrode material [36].

3.5. Stability study of PANI electrode

The cyclic voltammetric curves at the scan rate of 5 mV s^{-1} for the 1st and 2000th cycles are shown in Fig. 6. The specific capacitance value was calculated using the slowest scan rate i.e. 5 mV s^{-1}. The specific capacitance of polyaniline electrode decreased from 753 F g^{-1} to 592 F g^{-1} after the 2000 cycles. The polyaniline electrode exhibited 80% of initial capacity over 2000 cycles indicating the material suitability for energy-storage applications. Similarly, Dhawale et al. [33] reported stability up to 82% for electrosynthesis of PANI thin films for 1000 cycles. The specific and interfacial capacitance values are decreased by a small amount with the number of cycles due to the loss of active material caused by the dissolution and/or detachment, during the early charging and discharging cycles in the electrolyte.

3.6. Electrochemical impedance studies (EIS)

The electrical conductivity is the most important property of PANI and impedance measurements are used for conductivity studies as well as to elucidate mechanism and kinetics of the chemical and electrochemical reactions on PANI electrode [37]. In order to investigate the electrochemical characteristics of the electrode and electrolyte in quantitative manner impedance measurements were performed. The electrochemical impedance measurement (at open circuit voltage, in the frequency range 10^5 to 10^{-2} Hz) of polyaniline was carried out in 0.5 M H_2SO_4. The Nyquist depictions (Z' vs. Z'') of the raw impedance data for the PANI films on stainless steel substrate are shown in Fig. 7. For the convenience of the interpretation, this plot can be divided into high and low frequency regions. The frequency at which there is deviation from the semicircle is known as 'knee' frequency, which reflects the maximum frequency at which capacitive behavior is dominant. The presence of semicircle in the high frequency region suggests that the there is charge transfer resistance, while the straight line in the low frequency region angled of the ~45° to the real axis can be attributed to the capacitive behavior. Inset (Fig. 7) shows the expanded high frequency region of the same plot. This implies that the supercapacitor shows a blocking behavior at high frequencies and capacitive behavior at low frequencies [38–40]. The 20 Ω, high frequency impedance intercept reflects the equivalent series resistance (ESR) of the electrolyte [41,42]. The electrochemical parameters of the equivalent circuit were evaluated by employing the ZSimpWin software. Several equivalent circuits were tried to reproduce the Nyquist, Bode plots and the equivalent circuit shown in Fig. 8 was found to fit

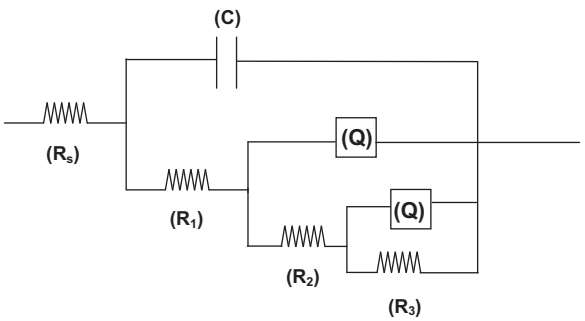

Fig. 8. Equivalent circuit model used to fit the electrochemical impedance data of PANI thin film.

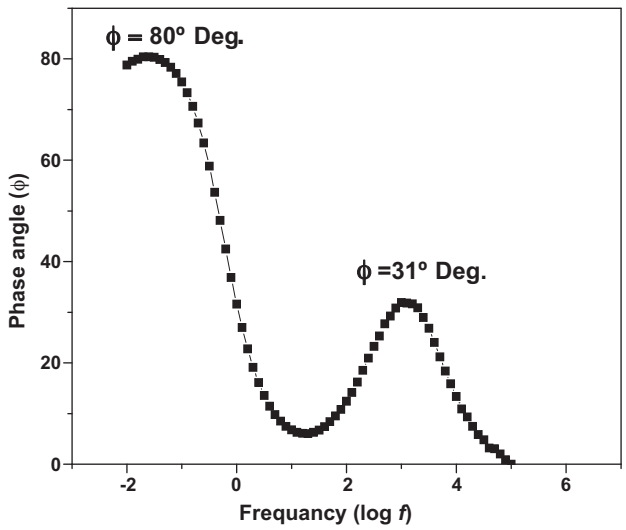

Fig. 9. Bode plot of PANI electrode in 0.5 M H_2SO_4 electrolyte.

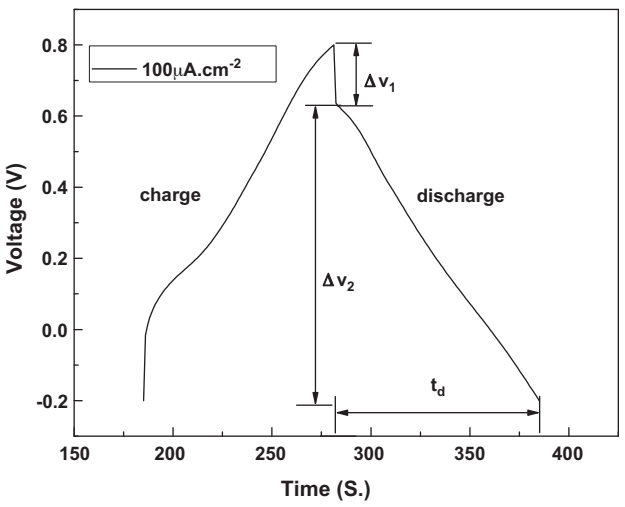

Fig. 11. Galvanostatic charge/discharge curve of PANI electrode recorded at constant current 100 μA cm^{-2} in 0.5 M H_2SO_4 electrolyte.

the experimental impedance data. In this model, 'R_S' is the solution resistance of the PANI and electrolyte, 'C' is the capacitance, 'R_1' is the resistance of the PANI film deposited on the substrate. The charge transfer and absorption resistance are denoted by R_2 and R_3, respectively. 'Q' is general imperfect capacitor when $n = 1$, $Q = C$ (capacitor), due to the semi-infinite diffusion of charges. 'Q' is one constant phase element that takes into account the interfacial irregularities such as porosity, roughness, and geometry.

Bode representation of this data is shown in Fig. 9. The Bode plot at a phase angle of 31° and 80° about 85% and 17% of the power corresponds to the heat production at the internal resistance. The loss factors of electrode 0.17 and 1.66 are calculated at frequencies 0.25 Hz and 1 kHz, respectively in the lower and higher frequency region. This is also in good agreement with the effect of scan rate on specific capacitance, wherein specific capacitance is higher for lower scan rate and it decreases for higher value. Therefore lower scan rate is appropriate for good performance of PANI electrode. The relaxation time constant (τ_0), can be calculated from plots of C' (ω) vs. frequency as shown in Fig. 10. Relaxation time (τ_0) for the PANI electrode is found to be 0.31 s. The τ_0 is a very important factor, which decides applicability of electrode material according to energy demand. Smaller relaxation time constant value exhibits a faster energy release capability of the electrode, to provide higher power density [41].

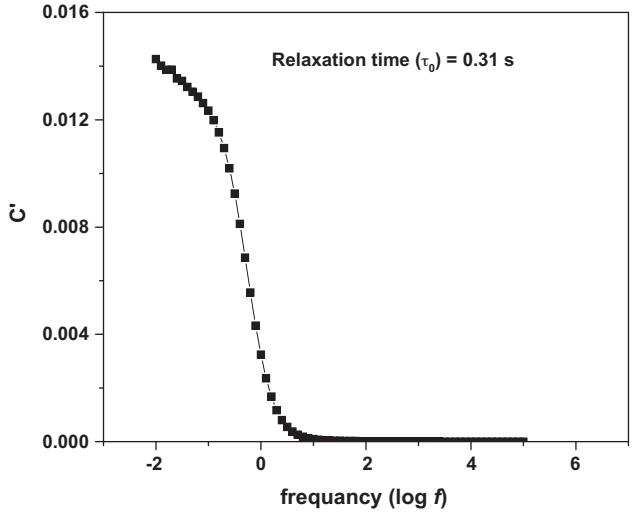

Fig. 10. Plot of real capacitance (C') vs. frequency for PANI electrode.

3.7. Charge/discharge study of PANI electrode

Charge/discharge behavior for supercapacitor made with PANI electrode is obtained at 100 μA cm^{-2} within the potential range of −0.2 to +0.8 V vs. SCE in 0.5 M H_2SO_4 is shown in Fig. 11. At the beginning of the charge and the discharge, we see a sharp change in voltage ΔV_1 due to the ESR of the supercapacitor, the t_d and ΔV_2 stands for the discharge time and voltage decrement, respectively [43]. A low current density was used in this study to allow the complete reaction between the electrolyte and the electrode. In the charge/discharge profile, the charging curves were not exactly symmetrical to the discharging curves. This implied that PANI electrode had small lacking of electrochemical reversibility and capacitive characteristics. During the experiments, the amount of charges stored in the capacitor was determined by integrating the current during charge and discharge time. At low discharge, potential response of the capacitor approached an ideal linear charge voltage relationship. At higher values of potential, the total impedance of the cell gave rise to an initial ohmic drop of the discharge voltage, which remained until constant capacitive performances are achieved. However, the initial decrease in capacitance is related to the irreversible charge compensation in faradaic reaction associated with the oxidation/reduction of PANI [43,44]. The electrochemical parameters such as specific power (SP) and specific energy (SE) are calculated using the following relationships [45].

$$\mathrm{SP} = \frac{I \times V}{m} \tag{4}$$

$$\mathrm{SE} = \frac{I \times t \times V}{m} \tag{5}$$

where SP is specific power in kW kg^{-1} and SE is specific energy in Wh kg^{-1}. The above expressions show the discharge current (I) in amperes, voltage range (V) in volts, discharge time (t) in seconds and mass of the electroactive material (m) in grams. The specific power and the specific energy from the charge/discharge plot were found to be 0.980 kW kg^{-1} and 28.3 Wh kg^{-1}, respectively.

4. Conclusions

In conclusion, the amorphous PANI thin films are prepared by the microwave assisted chemical bath deposition method

(MW-CBD). The mucky morphology is revealed from the SEM micrograph. The FT-IR spectrum confirmed the formation of PANI material. The PANI thin films are hydrophilic in nature with optical band gap of 2.5 eV. The PANI electrode showed maximum specific capacitance of 753 $F g^{-1}$ at low scan rate. The relaxation time constant 0.31 s is determined using electrochemical impedance spectroscopy studies. The specific power and specific energy estimated from the charge/discharge plot were found to be 0.980 $kW kg^{-1}$ and 28.3 $Wh kg^{-1}$, respectively.

Acknowledgement

Authors are also grateful to the Council for Scientific and Industrial Research (CSIR), New Delhi (India) for financial support through the scheme no. 03(1165)/10/EMR-II.

References

[1] Y.K. Srivastava, Rasayan J. Chem. 1 (2008) 884.
[2] R.S. Mane, C.D. Lokhande, Mater. Chem. Phys. 65 (2000) 1.
[3] D.P. Dubal, D.S. Dhawale, R.R. Salunkhe, V.J. Fulari, C.D. Lokhande, J. Alloys Compd. 497 (2010) 166.
[4] D.P. Dubal, D.S. Dhawale, R.R. Salunkhe, V.S. Jamdade, C.D. Lokhande, J. Alloys Compd. 492 (2010) 26.
[5] H. Mi, X. Zhang, S. An, X. Ye, S. Yang, Electrochem. Commun. 9 (2007) 2859.
[6] E. Vigil, D. Dixon, J.W.J. Hamilton, J.A. Byrne, Surf. Coat. Technol. 203 (2009) 3614.
[7] R. Zhai, S. Wang, H. Xu, H. Wang, H. Yan, Mater. Lett. 59 (2005) 1497.
[8] V.R. Shinde, C.D. Lokhande, R.S. Mane, S.H. Han, Appl. Surf. Sci. 245 (2005) 407.
[9] V.K. Ivanov, A.S. Shaporev, F.Y. Sharikov, A.Y. Baranchikov, Superlattices Microstruct. 42 (2007) 421.
[10] F. Wiesbrock, R. Hoogenboom, U.S. Schubert, Macromol. Rapid Commun. 25 (2004) 1739.
[11] V. Khomenko, E. Franckowiak, F. Beguin, Electrochim. Acta 50 (2005) 2499.
[12] K.S. Ryu, K.M. Kim, N.G. Park, Y.J. Park, S.H. Chang, J. Power Sources 103 (2002) 305.
[13] M.M. Ayad, N. Salahuddin, M.A. Shenashin, Synth. Met. 142 (2004) 101.
[14] E. Detsre, S. Thierry Dubas, J. Met. Mater. Miner. 19 (2009) 39.
[15] A.B. Afzal, M.J. Akhtar, M. Nadeem, M. Ahmad, M.M. Hassan, T. Yasin, M. Mehmood, J. Phys. D: Appl. Phys. 42 (2009) 015411.
[16] S. Sathiyanarayanan, S. Syed Azim, G. Venkatachari, Electrochim. Acta 52 (2007) 2068.
[17] C. Zhou, J. Han, G. Song, R. Guo, Macromolecules 40 (2007) 7075.
[18] R.C. Ramola, S. Chandra, J.M.S. Rana, R. Sharma, S. Annapoorni, R.G. Sonkawade, F. Singh, D.K. Avasthi, Curr. Sci. 97 (2009) 1453.
[19] S. Ivanov, P. Mokreva, V. Tsakova, L. Terlemezyan, Thin Solid Films 441 (2003) 44.
[20] R. Mazeikiene, A. Malinauskas, Synth. Met. 108 (2000) 9.
[21] D.S. Dhawale, D.P. Dubal, V.S. Jamadade, R.R. Salunkhe, C.D. Lokhande, Synth. Met. 160 (2010) 519.
[22] S.S. Joshi, C.D. Lokhande, J. Mater. Sci. 42 (2007) 1304.
[23] D.F. Li, W. Wang, H.J. Wang, X.S. Jia, J.Y. Wang, Appl. Surf. Sci. 255 (2008) 581.
[24] O. Bockman, T. Ostvold, G.A. Voyiatzis, G.N. Papatheodorou, Hydrometallurgy 55 (2000) 93.
[25] R.S. Mane, J. Chang, D. Ham, B.N. Pawar, T. Ganesh, B.W. Cho, J.K. Lee, S.H. Han, Curr. Appl. Phys. 9 (2009) 87.
[26] H. Zengin, W. Zhou, J. Jin, R. Czerw, D.W. Smith, J.L. Echegoyen, D.L. Carroll, S.H. Foulger, J. Ballato, Adv. Mater. 14 (2002) 1480.
[27] Y. Tan, Y. Zhang, J. Kan, eXPRESS Polym. Lett. 3 (2009) 333.
[28] J.J. Lunhong, L.C. Li, J. Mater. Sci. 44 (2009) 1024.
[29] M.R. Saboktakin, A. Maharramov, M.A. Ramazanov, Nat. Sci. 5 (2007) 67.
[30] A. Tiwari, V. Singh, eXPRESS Polym. Lett. 1 (2007) 308.
[31] S.S. Joshi, T.P. Gujar, V.R. Shinde, C.D. Lokhande, Sens. Actuators B 132 (2008) 349.
[32] J.N. Broughton, M.J. Brett, Electrochem. Solid State Lett. 5 (2002) 279.
[33] D.S. Dhawale, R.R. Salunkhe, V.S. Jamadade, D.P. Dubal, S.M. Pawar, C.D. Lokhande, Curr. Appl. Phys. 10 (2010) 904.
[34] V. Gupta, N. Miura, Electrochem. Solid State Lett. 8 (2005) 630.
[35] V.S. Jamadade, D.S. Dhawale, C.D. Lokhande, Synth. Met. 160 (2010) 955.
[36] T.P. Gujar, W.Y. Kim, I. Puspitasari, K.D. Jung, O.S. Joo, Int. J. Electrochem. Sci. 2 (2007) 666.
[37] A. Sezai Sarac, M. Ates, B. Kilic, Int. J. Electrochem. Sci. 3 (2008) 777.
[38] G. Arabale, D. Wagh, M. Kulkarni, I.S. Mulla, S.P. Vernekar, K. Vijayymohanan, A.M. Rao, Chem. Phys. Lett. 376 (2003) 207.
[39] M.S. Dandekar, G. Arabale, K. Vijayymohanan, J. Power Sources 141 (2005) 198.
[40] W.C. Chen, T.C. Wen, H. Teng, Electrochem. Acta 48 (2003) 641.
[41] V. Ganesh, S. Pitchumani, V. Lakshminarayanan, J. Power Sources 158 (2006) 1523.
[42] X.F. Wang, D.B. Ruan, D.Z. Wang, J. Liang, Acta Phys. Chem. Sin. 21 (2005) 261.
[43] F. Pico, J. Ibanez, M.A. Lillo-Rodenas, A. Linares-Solano, R.M. Rojas, J.M. Amarilla, J.M. Rojo, J. Power Sources 176 (2008) 417.
[44] S. Richard Prabhu Gnanakan, M. Rajasekhar, A. Subramania, Int. J. Electrochem. Sci. 4 (2009) 1289.
[45] K. Prasad, N. Munichandraiah, Electrochem. Solid State Lett. 5 (2002) 271.